

# The study of the elliptical complex geometry orientation effect on the natural convection of hybrid nanofluid under the influence of uniform magnetic field

Mohamed Boucetta<sup>1\*</sup>, Zoubair Boulahia<sup>2</sup>, Ahmed Hader<sup>1</sup>, and F.Z. Krimech<sup>1</sup>

1 Hassan II University, Higher Normal School, Interdisciplinary Laboratory of Fundamental and Applied Sciences, Casablanca, Morocco

2 Hassan II University, Faculty of Sciences Aïn Chock, Laboratory of Mechanics, BP 5366 Maarif, 20100 Casablanca, Morocco

**Abstract.** In this study, natural convection under the influence of a magnetic field was investigated via simulation in a square cavity with thermally insulated horizontal walls and a cold vertical wall, containing an elliptical heat source at different angles ( $\theta = 0^\circ$ ,  $\theta = 45^\circ$ ,  $\theta = 90^\circ$ ) surrounded by a hybrid nanofluid consisting of titanium dioxide, copper and water. The Simple algorithm and the finite volume method were then employed to solve the equations. This study examined the effect of the Rayleigh number (Ra), the Hartmann number (Ha), and the volume fraction of particles ( $\varphi$ ) in the medium on fluid motion and heat transfer. The results obtained for streamlines and isotherms at different  $\theta$  orientations of the heated body show that the orientation of the ellipsoidal mass has a significant effect on thermal performance. These results provide important information for a better understanding of the design of cooling systems in the presence of a magnetic field.

**Keywords:** MHD natural convection; Orientations; Elliptical Heater.

## 1 Introduction

Convection of nanofluids in containers holding a heat source element is a crucial process due to its numerous applications, and its importance increases with the addition of nanomaterials that enhance heat transfer efficiency. These applications include: cooling electronic devices and storing thermal energy, room ventilation using chillers, cooling containers and heat exchangers, and heating and cooling systems in nuclear reactors. One of the earliest attempts to statistically model natural convection within cavities was the pioneering work of De Val Davis [1]. Boucetta et al. [2] studied the free convection of a TiO<sub>2</sub>-Cu-Water within a square cavity containing a centric elliptical heat block. Discretization was performed using finite

---

\* Corresponding author: [mohamed.boucetta1-etu@etu.univh2c.ma](mailto:mohamed.boucetta1-etu@etu.univh2c.ma)

volumes and the algorithm SIMPLE. The results revealed that the total heat transfer rate increases with the Rayleigh number ( $Ra$ ) from  $10^3$  to  $10^6$ , reaching a vertical peak for  $Ra$  values between  $10^4$  and  $10^6$ . Furthermore, the maximum flow rate of the nanofluid is observed for  $Ra = 10^6$ , with optimal heat transfer occurring at a nanoparticle volume percentage of 5%. R. H. Hameed et al. [3] studied optimizing heat transfer with casson-based Cu-H<sub>2</sub>O nanofluids to enhance free convection using numerical simulations and the Galerkin finite element method. They evaluated various factors like Rayleigh number and Casson fluid parameter, finding that higher Rayleigh numbers and Casson parameters improved heat transfer significantly, increasing the average Nusselt number by up to 165%. An optimal range of corrugation numbers for efficiency was identified, and nanoparticles improved the average Nusselt number by 20% at a Rayleigh number of 105, contributing to efficient thermal management in electronics cooling and solar collectors. G. Yan et al. [4] conducted an in-depth investigation of hot, oval-shaped porous media in a container filled with ethylene glycol under a magnetic field. They discovered that the Hartmann number reduces heat transfer. A. Boulahia et al. [5] examined in detail a study of the effect of container surface movement on heat transfer through nanofluids, concluding that heat transfer could be effectively controlled by adding heated micro-particles and regulating their positions. S. S. Billah et al. [6] analyzed the numerical simulation of free convection flow in a square enclosure featuring elliptic blockages. It described a setup with a heated bottom wall, insulated side walls, and a cool top wall, focusing on the effects of varying Rayleigh numbers on fluid flow and temperature gradients at different blockage locations. The main objective of this work is to analyze the natural convection heat transfer phenomenon of a hybrid nanofluid in a square container containing an ellipse with different orientations. Numerical results from previous studies are used to validate the calculation method presented in this article. We investigated the effects of the Hartmann number  $Ha$  and number of the Rayleigh number ( $Ra$ ) and the nanoparticle volume fraction ( $\phi$ ). Brinkman-Maxwell. [7,8] model of effective viscosity and thermal conductivity were established [7,8] to evaluate the physical properties of the hybrid nanofluid. To demonstrate the interaction between the hybrid nanofluid and the heating element surface, we present our numerical results in the form isotherms, streamlines, and average Nusselt numbers.

## 2 Statement of Problem

Figure 1 illustrates the coordinate systems and configuration under investigation. The right and left walls of the cavity are at a constant low temperature ( $T_c$ ), whilst the other walls are insulated. The ellipsoidal body is heated at ( $T_h$ ) and at varying angles. The average temperature of the fluid,  $(T_c + T_h)/2$ , was calculated for the physical and thermal properties shown in Table 1.

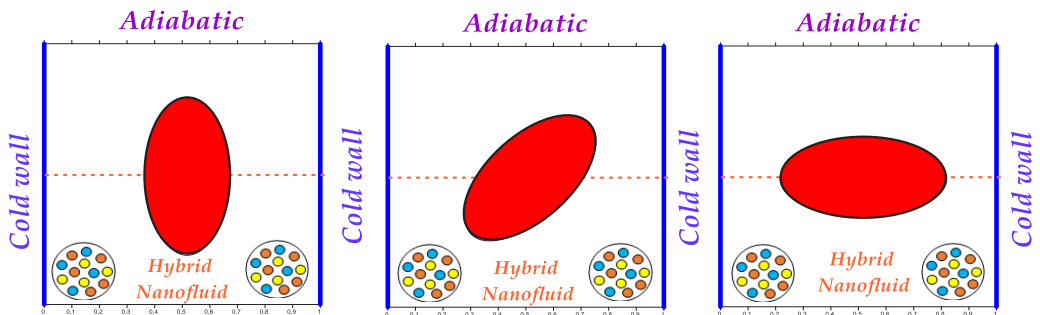


Fig. 1. A diagram illustrating the boundary conditions for a cavity containing a heat source at its center.

**Table 1:** Characteristics of water and nanoparticles [9]

	$C_p$ (J /Kg K)	$\rho$ (Kg /m <sup>3</sup> )	$K$ (w /mK)	$\beta$ (K <sup>-1</sup> )	$\mu$ × 10 <sup>6</sup> (kg m <sup>-1</sup> s <sup>-1</sup> )	$d_p$
(TiO <sub>2</sub> )	710	4157	8.4	0.9 × 10 <sup>5</sup>	–	25
(H <sub>2</sub> O)	4179	997.1	0.613	27.6 × 10 <sup>5</sup>	855	0.385
(Cu)	386	8934	402	1.66 × 10 <sup>5</sup>	–	26

### 3 Formulation in mathematics

The fundamental equations of flow in two dimensions are expressed as follows [2]:

$$\frac{\partial u}{\partial x} + \frac{\partial v}{\partial y} = 0 \tag{1}$$

$$u \frac{\partial u}{\partial x} + v \frac{\partial u}{\partial y} = -\frac{1}{\rho_{nf}} \frac{\partial p}{\partial x} + \frac{\mu_{nf}}{\rho_{nf}} \left( \frac{\partial^2 u}{\partial x^2} + \frac{\partial^2 u}{\partial y^2} \right) \tag{2}$$

$$u \frac{\partial v}{\partial x} + v \frac{\partial v}{\partial y} = -\frac{1}{\rho_{nf}} \frac{\partial p}{\partial y} + \frac{\mu_{nf}}{\rho_{nf}} \left( \frac{\partial^2 v}{\partial x^2} + \frac{\partial^2 v}{\partial y^2} \right) + \frac{(\rho\beta)_{nf}}{\rho_{nf}} (T - T_c) - \sigma_{nf} B_0^2 v \tag{3}$$

$$u \frac{\partial T}{\partial x} + v \frac{\partial T}{\partial y} = \alpha_{nf} \left( \frac{\partial^2 T}{\partial x^2} + \frac{\partial^2 T}{\partial y^2} \right) \tag{4}$$

Regarding the equations for the thermophysical properties of the nanofluid [10]:

$$\rho_{nf} = (1 - \varphi)\rho_f + \varphi_{TiO_2}\rho_{TiO_2} + \varphi_{Cu}\rho_{Cu} \tag{5}$$

$$(\rho C_p)_{nf} = (1 - \varphi)(\rho C_p)_f + \varphi_{TiO_2}(\rho C_p)_{TiO_2} + \varphi_{Cu}(\rho C_p)_{Cu} \tag{6}$$

$$(\rho\beta)_{nf} = (1 - \varphi)(\rho\beta)_f + \varphi_{TiO_2}(\rho\beta)_{TiO_2} + \varphi_{Cu}(\rho\beta)_{Cu} \tag{7}$$

$$\alpha_{nf} = k_{nf}/(\rho C_p)_{nf} \tag{8}$$

The model of Brinkman-Maxwell [7,8] for the conductivity and viscosity are given by:

$$\mu_{nf} = \frac{\mu_f}{(1 - \varphi)^{2.5}} \tag{9}$$

$$k_{nf} = \frac{k_s \cdot k_f + 2k_f^2 - 2(k_f - k_s)k_f \varphi}{k_s + 2k_f + (k_f - k_s)\varphi} \tag{10}$$

The boundary conditions for the phenomenon of natural convection are as follows:

$$\begin{aligned} u = 0, \quad v = 0, \quad \frac{\partial T}{\partial y} = 0 & \quad \text{Bottom} \\ u = 0, \quad v = 0, \quad \frac{\partial T}{\partial y} = 0 & \quad \text{Top} \\ u = 0, \quad v = 0, \quad T = T_c & \quad \text{Right-hand} \\ u = 0, \quad v = 0, \quad T = T_c & \quad \text{Left-hand} \end{aligned} \tag{11}$$

The dimensionless variables for natural convection, derived from the properties of a pure fluid, are as follows:

$$X = \frac{x}{H}, \tau = \frac{t}{H/U_{ref}}, \quad Y = \frac{y}{H}, V = \frac{v}{U_{ref}}, U = \frac{u}{U_{ref}}, P = \frac{p}{\rho_{nf}U_{ref}^2}, \theta = \frac{T - T_c}{T_h - T_c} \tag{12}$$

$U_{ref}$  represents  $\alpha_f/H$  under normal convective conditions. The non-standard numbers in the system are interpreted as follows:

$$Gr = \frac{g\beta_f(T_h - T_c)H^3}{\nu_f^2}, Ra = Gr.Pr, Ha = HB_0\sqrt{\sigma_f/\mu_f} \tag{13}$$

$$Ra = \frac{g\beta_f(T_h - T_c)H^3}{\alpha_f\nu_f}, Pr = \frac{\nu_f}{\alpha_f} \tag{14}$$

The governing equations in the non-dimensional form (1) to (4) [2]:

$$\frac{\partial U}{\partial X} + \frac{\partial V}{\partial Y} = 0 \tag{15}$$

$$U \frac{\partial U}{\partial X} + V \frac{\partial U}{\partial Y} = -\frac{\partial P}{\partial X} + Pr \frac{\rho_f \mu_{nf}}{\rho_{nf} \mu_f} \left( \frac{\partial^2 U}{\partial X^2} + \frac{\partial^2 U}{\partial Y^2} \right) \tag{16}$$

$$U \frac{\partial V}{\partial X} + V \frac{\partial V}{\partial Y} = -\frac{\partial P}{\partial Y} + Pr \frac{\rho_f \mu_{nf}}{\rho_{nf} \mu_f} \left( \frac{\partial^2 V}{\partial X^2} + \frac{\partial^2 V}{\partial Y^2} \right) + Ra.Pr \frac{(\rho\beta)_{nf}}{\rho_{nf}\beta_f} \theta - \frac{\rho_f \sigma_{nf}}{\rho_{nf} \sigma_f} Ha^2 Pr V \tag{17}$$

$$U \frac{\partial \theta}{\partial X} + V \frac{\partial \theta}{\partial Y} = \frac{\alpha_{nf}}{\alpha_f} \left( \frac{\partial^2 \theta}{\partial X^2} + \frac{\partial^2 \theta}{\partial Y^2} \right) \tag{18}$$

Unmeasured variables related to boundary conditions are written in this form:

$$\begin{aligned} U = 0, \quad V = 0, \quad \frac{\partial \theta}{\partial Y} = 0 & \quad \text{Bottom} \\ U = 0, \quad V = 0, \quad \frac{\partial \theta}{\partial Y} = 0 & \quad \text{Top} \\ U = 0, \quad V = 0, \quad \theta = 0 & \quad \text{Right-hand} \\ U = 0, \quad V = 0, \quad \theta = 0 & \quad \text{Left-hand} \end{aligned} \tag{19}$$

This represents of average value of the Nusselt coefficient for the entire cavity wall:

$$\overline{Nu}_{tot} = \frac{1}{H} \int_0^H \frac{k_{nf}(\varphi)}{k} \left\{ \left| \frac{\partial \theta}{\partial X} \right|_{left} + \left| \frac{\partial \theta}{\partial X} \right|_{right} \right\} dy \tag{20}$$

## 4 Numerical details

Based on the finite volume method highlighted by Patanakar [11], and following the derivation of Equation (19) and the governing equations (15) to (18), whilst utilising Spalding’s hybrid differential scheme (HDS) to solve the heat transfer equations, and the Simple method to solve and correct the pressure and velocity equations, the triangular matrix algorithm (TDMA) [12] was highlighted in detail. The methodology studied was implemented using a Fortran code.

### 4.1 Independence from the grid

To find an appropriate grid for simulation, we used a square cavity with vertically oriented heat sources with an orientation of  $\theta=90^\circ$  and a hybrid nanofluid of water, copper, and titanium dioxide ( $\varphi=5\%$ ) and a central heat source with a coefficient  $r=a/H=0.3$  at two extreme Rayleigh number values ( $Ra=10^4, Ra=10^6$ ). For the Nusselt number for a variety of mesh numbers is shown in Table 2. The table below makes it clear that the  $101 \times 101$  mesh is sufficient for numerical calculations.

**Table 2:** The effect of mesh size on (Nu) is investigated using an elliptical heat source at the centre with  $r = 0.30$  at ( $\varphi = 5\%$ ).

<i>Ra</i>	$63 \times 63$	$83 \times 83$	$103 \times 103$	$123 \times 123$
$10^4$	6.071	6.543	6.679	6.681
$10^6$	20.951	21.411	21.650	21.682

### 4.2. Validations

A number of references were used to assess the validity of the numerical method presented. Deval Davis [2] studied a benchmark problem concerning spontaneous heat transfer within a cube-shaped cavity containing air. The mean Nusselt number of the present results was compared with the numerical data presented in [13–14] shown in Table 3. In the second case, there is a circle heating source inside a cubic cavity. The isothermal and streamline lines were then compared with those published by Park et al. [15] in Figure 2.

**Table 3:** Points of comparison regarding ( $\bar{Nu}$ ) between the current results and those reported in the literature, taking into account the variation in the Rayleigh number Ra.

Rayleigh number	$10^3$	$10^4$	$10^5$	$10^6$
Markatos et al [13]	1.114	2.238	4.509	8.754
Vahl Davis [1]	1.118	2.243	4.519	8.799
Fusegi et al [14]	1.118	2.245	4.521	8.825
Current study	<b>1.118</b>	<b>2.242</b>	<b>4.480</b>	<b>8.683</b>
Grid size	83*83	83*83	83*83	103*103

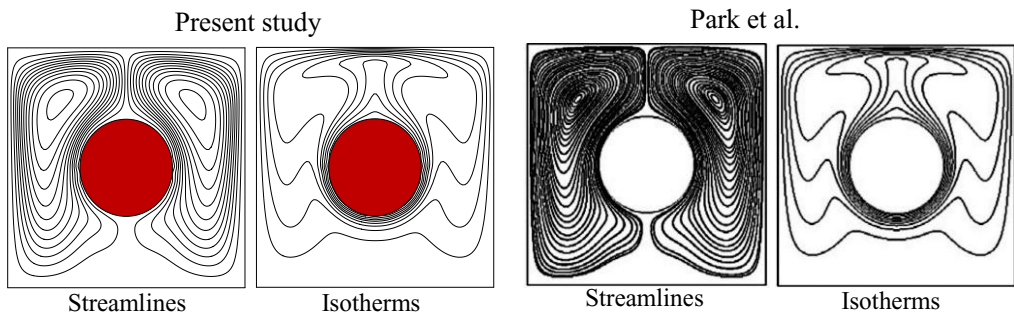


**Fig. 2.** Flow lines and isotherms between the present study and the study by Park et al. [15].

## 5 Results and discussion

In this research, we report the main numerical findings about how the free convection phenomenon in a square cavity filled with a hybrid nanofluid of water, copper, and titanium dioxide with a central heating element is affected by a uniform magnetic field, the Rayleigh number, and the nanoparticle size ratio. This section's goal is to investigate how heat transfer inside the cavity is impacted by the strength of the magnetic field and the previously mentioned variables. Numerical simulations were performed for Hartmann numbers Ha (0, 45), different hybrid nanofluid volume ratios (0, 5%), Rayleigh numbers Ra ( $10^3$ ,  $10^4$ ), and several orientations of the heated ellipse  $\theta$  ( $0^\circ$ ,  $45^\circ$ ,  $90^\circ$ ). The results of the Nusselt number, flow lines, and temperature fields are displayed.

### 5.1 Effect of Rayleigh

Figure 3 represents the distribution of flow lines and isotherms within the container at various values of Ra and  $\theta$ . In general, Figure 3 illustrates how two vortices, one on the left and one on the right, determine the flow structure of the TiO<sub>2</sub>-Cu-water hybrid nanofluid. The shapes of these two vortices vary depending on the angle of the central heat source. When Ra =  $10^3$ , conduction is the dominant mode. We find that as  $\theta$  increases at a volume fraction of  $\phi = 5\%$

of the hybrid nanofluid, the value of the maximum of the flow function increases from  $\theta = 0^\circ$  to  $\theta = 90^\circ$ . The figures shown in Figure 3 correspond to the maximum value of the flow function, which is optimal at  $\theta = 45^\circ$ . Conversely, the heat transfer rate declines as the rotation angle of the ellipsoid increases, and thermal conductivity improves when the angle is  $\theta = 0^\circ$ . The value of the maximum fluid flow function for the hybrid nanofluid and the heat transport rate reach their maximum at an angle of  $\theta = 0^\circ$  when the heated elliptical body is in a vertical position, which remains ideal for natural convection, where  $\theta$  increases from  $\theta = 0^\circ$  to  $\theta = 90^\circ$  when natural convection driven by conduction prevails at  $Ra = 10^6$ .

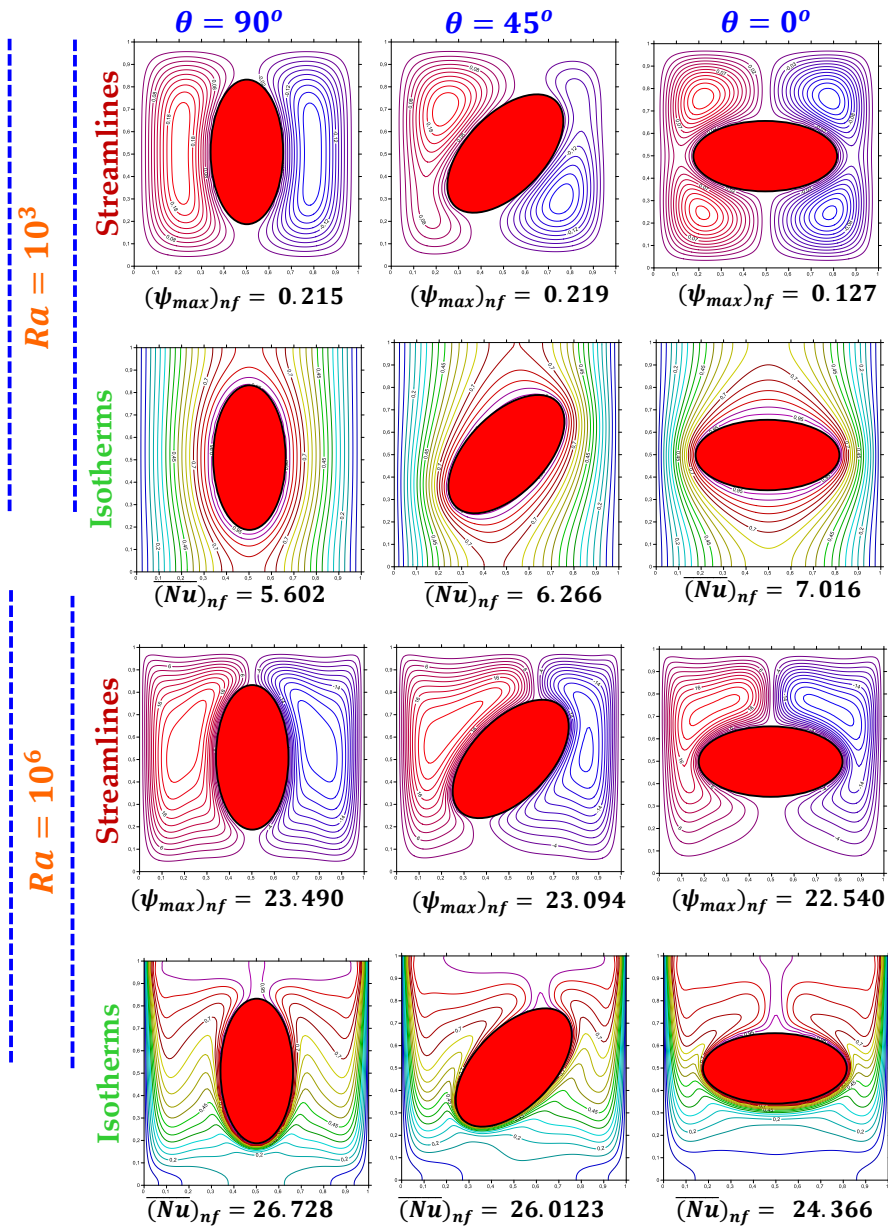


**Fig. 3.** The streamline and isothermal lines within the cavity containing a heated ellipsoidal segment, of a hybrid nanofluid with a  $\phi = 5\%$  fraction, with varying values of  $Ra$ ,  $\theta$  and  $Ha = 0$ .

### 5.2 Effect of Hartmann

When there is no magnetic field, when Ha is 0 and Ra is 106, flow occurs via natural convection. As shown in Figure 4, as  $\theta$  increases from  $\theta = 0^\circ$  to  $\theta = 90^\circ$ , the peak value of the flow rate function increases, reaching its maximum at  $\theta = 90^\circ$ . We also note that the thermal transfer rate also increases with the rotation angle and reaches its maximum at  $\theta = 90^\circ$ .

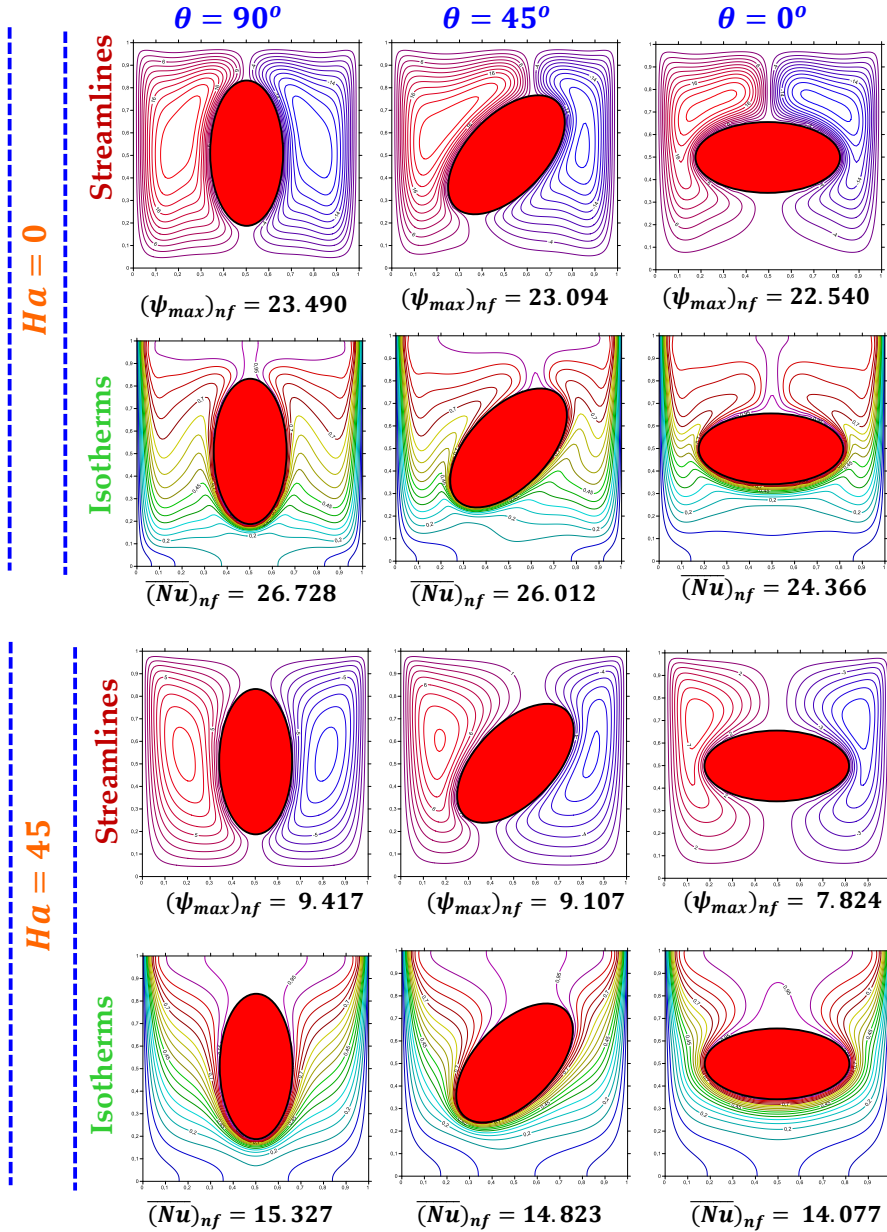


**Fig. 4.** The Streamline and isothermal in the cavity containing a heated ellipse, in the case of a hybrid nanofluid with  $\phi=5\%$  fraction for Ha and  $\theta$  different and Ra=106.

As for the Hartmann number effect, when moving from  $Ha = 0$  to  $Ha = 45$ , natural convection dominates. We find that the values of the current function are strongly dependent on the Lorentz force of the magnetic field, reducing the flow velocity from 23.490 to 9.417 at  $\theta = 90^\circ$  and the heat transport rate from 26.728 to 15.327. In this case, when the Hartmann number is high, the values of the current function increase gradually with increasing angle, and from Figure 4, we can see that when  $Ha = 45$ , the heat transfer number  $Nu$  decreases compared to  $Ha = 0$ , indicating that heat transfer becomes lower; and heat transfer is highest in this case for the angle  $\theta = 90^\circ$ , compared to the values for the other directions.

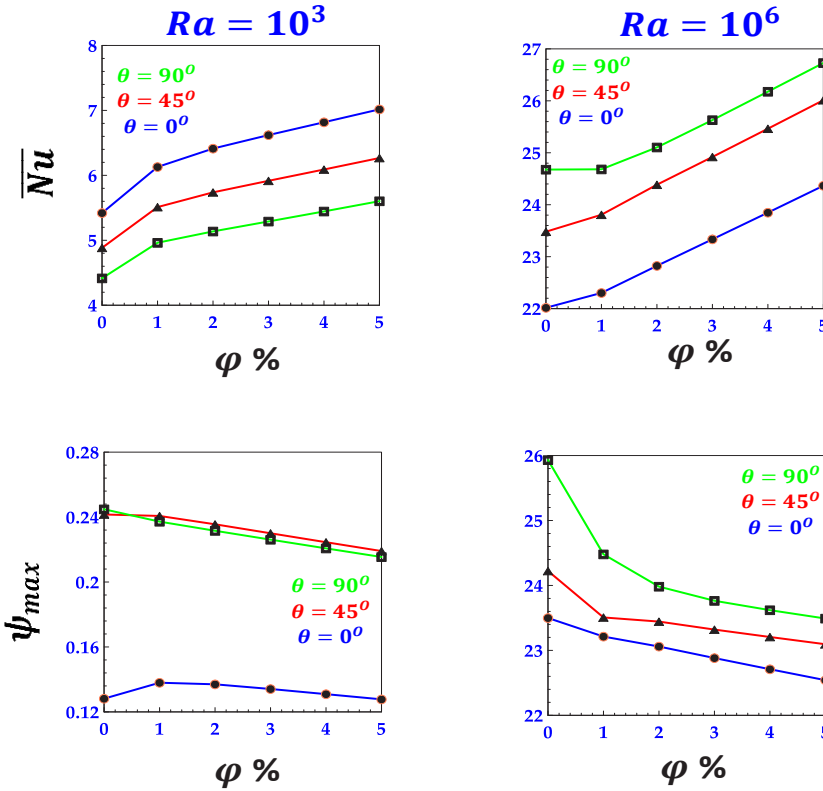


**Fig. 5.** Nusselt number  $\overline{Nu}$  and  $\psi_{max}$  as a function of  $\phi$  inside the cavity containing a heated ellipse, in the case of a hybrid nanofluid for  $\theta$ ,  $Ra=10^6$ ,  $Ra=10^3$  and  $Ha=0$ .

Figure 5 shows the variation in the Nusselt number ( $\overline{Nu}$ ) and the peak value of the stream function ( $\psi_{max}$ ) as a function of the concentration of  $TiO_2$ - $Cu$ -water hybrid nanoparticles. When  $Ra$  is low ( $Ra = 10^3$ ), the heat transfer coefficient increases unevenly as the concentration of  $TiO_2$ - $Cu$ -water hybrid nanoparticles in the medium rises, reaching its maximum value at  $\phi = 5\%$ . Conversely, as  $Ra$  increases, the thermal transfer rate rises significantly compared to the previous case, reaching its highest value at  $\phi = 5\%$ . It was also noted that the thermal transfer rate increases as the rotation angle of the heated elliptical shape decreases from  $a = 90^\circ$  to  $0^\circ$ . With regard to the streamlines, the increase in nanoparticles in the water leads to improved viscosity, which is the direct cause of the reduced maximum current value shown in Figure 5. It is worth noting in Figure 5 that changing the angle of the heating source from  $\theta = 0^\circ$  to  $90^\circ$  increases the peak value of the stream function at  $Ra =$

$10^3-10^6$ , which is significant for the angle  $\theta = 90^\circ$  when the elliptical body is perpendicular compared to other directions.

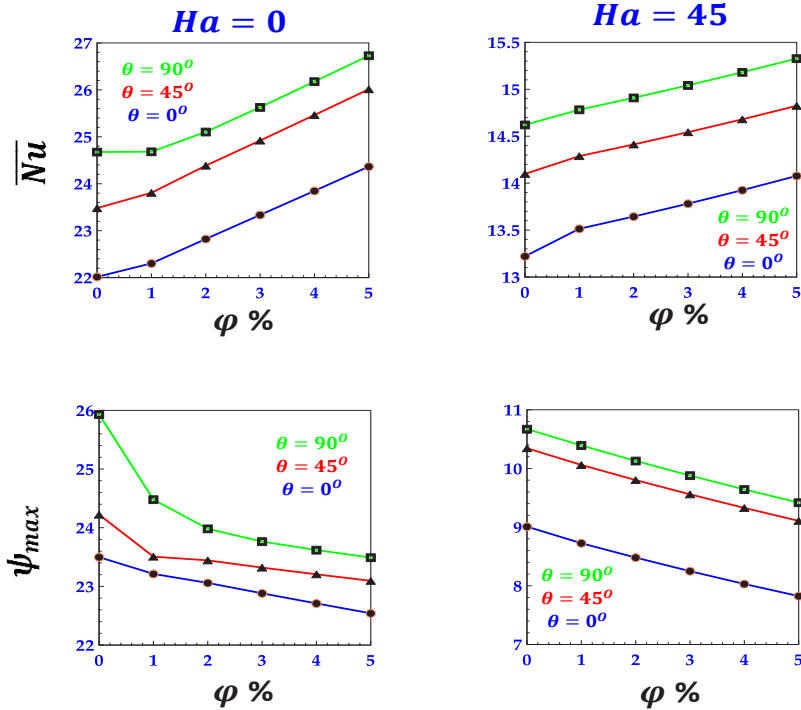


**Fig. 6.** Nusselt number  $\overline{Nu}$  and  $\psi_{max}$  as a function of  $\varphi$  inside the cavity containing a heated ellipse, in the case of a hybrid nanofluid of  $Ha=0$ ,  $Ha=45$ ,  $\theta$  and  $Ra=10^6$ .

Figure 6 shows that in the case where there is no magnetic field, the addition of nanoparticles to water results in an improvement in heat conduction efficiency within the vessel, reaching a maximum of  $\varphi=5\%$ , owing to an increase in the heat conductivity, where it is most effective at an angle of  $\theta=90^\circ$ . As for the current function, it decreases with an increase in nanoparticles in the cavity, as observed in Figure 6, such that the flow velocity is low. However, in the magnet field at  $Ha$  is 45, it can be seen from Figure 6 that the current function decreases significantly compared to the absence of a magnet field. This is due to the convergence of the flow lines and the reduction in flow velocity in the magnetic field. Furthermore, it is also known that the heat transfer rate decreases in the presence of the Lorentz drag force. We also conclude that, in the absence or presence of the magnetic field, the angle  $\theta = 90^\circ$  is superior to the other angles in terms of the rate of convective heat transfer.

## 6 Conclusion

In this study, the process of free convection was modelled in a cavity filled with a hybrid nanofluid and an elliptical heat source. The following conclusions were drawn from the results:

- Vortex cells, which characterise the flow structure of the hybrid nanofluid composed of titanium dioxide and copper, are the dominant pattern at high Rayleigh numbers  $Ra$ . The fluid flow function is at its best at a rotation angle of  $\theta = 45^\circ$ , and the rate of heat transfer

decrease with increasing rotation angle. At a rotation angle of  $\theta = 90^\circ$ , natural convection prevails.

- The stream function and thermal transfer rate increase with the rotation angle, reaching their peak values at  $\theta = 90^\circ$ . The Lorentz force of the magnetic field affects the flow field and the thermal transfer rate, with the thermal transfer rate reaching its highest levels at a rotation angle of  $\theta = 90^\circ$ .
- The heat transfer rate using hybrid nanoparticles increases at the low Rayleigh values ( $Ra = 10^3$ ) and improves at the high Rayleigh values ( $Ra = 10^6$ ), peaking at 5%. The nanoparticles also improve viscosity, leading to a decrease in the flow function.
- In the absence of a magnetic field, the adding of nanoparticles to water enhances thermal transfer efficiency, reaching a maximum value of  $\phi = 5\%$ . However, in the presence of a magnetic field, the flow function decreases because of the convergence of the flow lines.

## References

1. G. De Vahl Davis, Natural convection of air in a square cavity: a bench mark numerical solution, *Int. J. Numer. Methods Fluids* 3 (1983) 249–264, <https://doi.org/10.1002/flid.1650030305>
2. BOUCETTA, Mohamed, BOULAHIA, Zoubair, EJRAYDI, Manal, et al. Free convection within a container having hybrid water nanofluid with elliptical heater with different orientation. *Multidiscipline Modeling in Materials and Structures*, 2025, vol. 21, no 6, p. 1331-1341.
3. R. H. Hameed et al., “Free convection investigation for a Casson-based Cu–H<sub>2</sub>O nanofluid in semi parabolic enclosure with corrugated cylinder,” *Heliyon*, 2025, doi:10.1016/j.heliyon.2024.e40960.
4. G. Yan, A. Shawabkeh, R. Chaturvedi, R. Nur-Firyal, and M. Mehdizadeh Youshanlouei, “Using MHD free convection to receive the generated heat by an elliptical porous media,” *Case Studies in Thermal Engineering*, 2022, doi: 10.1016/j.csite.2022.102153.
5. Boulahia, Z., Wakif, A., Sehaqui, R.: Numerical study of mixed convection of the nanofluids in twosided lid-driven square cavity with a pair of triangular heating cylinders. *J. Eng.* (2016). <https://doi.org/10.1155/2016/8962091>.
6. S. S. Billah et al., “Free convection at different locations of adiabatic elliptic blockage in a square enclosure,” *Mathematical Modelling and Numerical Simulation with Applications*, 2024, doi:10.53391/mmnsa.1382516.7. [https://doi.org/10.21272/jnep.15\(5\).05032](https://doi.org/10.21272/jnep.15(5).05032)
7. J.C. Maxwell. *A Treatist on electricity and Magnetism*, second ed. Oxford University Press. Cambridge. (1904), pp. 435–441, *A Treatise on Electricity and Magnetism* - James Clerk Maxwell - Google Livres
8. H.C Brinkman, the viscosity of concentrated suspensions and solutions, *journal of chemical physics* 20 (1952) 571–581, 10.1063/1.1700493
9. F.P. Incropera, D.P. DeWitt, *Introduction to Heat Transfer*, Wiley, New York, 2002.
10. Z. Haddad, H.F. Oztop, E. Abu-Nada, A. Mataoui, A review on natural convective heat transfer of nanofluids, *Renewable Sustainable Energy Rev.* 16 (2012) 5363–5378, <https://doi.org/10.1016/j.rser.2012.04.003>
11. S.V. Patankar, *Numerical Heat Transfer and Fluid Flow*, McGraw-Hill, Washington, (1980), <https://doi.org/10.1201/9781482234213>
12. D.B. Spalding, A novel finite difference formulation for differential expressions involving both first and second derivatives, *Int. J. Numer. Methods Eng.* 4 (1972) 551–559, <https://doi.org/10.1002/nme.1620040409>

13. N.C. Markatos, K.A. Pericleous, "Laminar and turbulent natural convection in an enclosed cavity", *International Journal of Heat and Mass Transfer*, Vol. 27, No. 5, pp. 755–772, 1984. [https://doi.org/10.1016/0017-9310\(84\)90145-5](https://doi.org/10.1016/0017-9310(84)90145-5)
14. T. Fusegi, J.M. Hyun, K. Kuwahara, B. Farouk, "A numerical study of three-dimensional natural convection in a differentially heated cubical enclosure", *International Journal of Heat and Mass Transfer*, Vol. 34, No. 6, pp. 1543–1557, 1991. [https://doi.org/10.1016/0017-9310\(91\)90295-P](https://doi.org/10.1016/0017-9310(91)90295-P)
15. Park HK, Ha MY, Yoon HS, Park YG, Son C. A numerical study on natural convection in an inclined square enclosure with a circular cylinder. *Int J Heat Mass Transf* (2013): 66:295-314, <https://doi.org/10.1016/j.ijheatmasstransfer.2013.07.029>